2005 WSEAS Int. Conf. on DYNAMICAL SYSTEMS and CONTROL, Venice, Italy, November 2-4, 2005 (pp142-147)

# Heart Rate Variability Spectral Analysis Using Quadratic Time-Frequency Representations

EUGEN R. LONTIS [(1)] and ANASTASIOS G. BEZERIANOS [(2)]

[(1)] Center for Sensory Motor Interaction (SMI),
Aalborg University,
Fredrik Bajers Vej 7, D3, 9220 Aalborg Øst
DENMARK.

[(2)] Medical Physics Department, School of Medicine,
Patras University,
GREECE.

*Abstract* - Time frequency representations (TFR) have been assessed with respect to time and frequency resolution using a simulated and real heart rate variability data, HRV. The Wigner-Ville Distribution proved to have a difficult interpretation due to the presence of the cross-terms. Choi-Williams, CW, and Signal-dependent radially Gaussian kernel, SD, TFRs used different techniques for cross-terms suppression and had comparative results due to the auto-terms geometry around the center in the ambiguity domain, with a trade-off between cross-terms suppression and auto-terms smoothing. An elevated vagal and a reduced sympathetic activity in the clinostatic position, and a reduced vagal and elevated sympathetic activity in the orthostatic position, respectively, have been detected in HRV by CW and SD during the tilt-up test.

*Key-Words*: time-frequency representations, HRV, myocardial infarction, autonomic nervous system

## 1 Introduction

Noninvasive techniques are more often employed in assisting the medical diagnosis. Heart rate variability analysis provides important markers in the assessment of the autonomic nervous system. The importance of this analysis is emphasized by the efforts done for standardization of measurement, physiological interpretations and clinical use [1].

Studies performed in the cases of myocardial infarction [5], [8], diabetic cardiac autonomic neuropathy [4], cardiac transplant [1], hypovolemic shock [1], respectively in the case of the autonomic nervous system tests [2], have distinguished the pathological or physiological states of the autonomic nervous system reflected in the spectral analysis.

Heart rate variability is the result of the action of complex neural control mechanisms [1], [3], [5]. The role of these mechanisms is to maintain the controlled parameters within physiological range. Cardiac control mechanisms influence in a high degree the pattern of the HRV by efferent sympathetic and vagal activities directed to the sinus node. Largely synchronous with each cardiac cycle, the sinus node discharge can be modulated by central, vasomotor and respiratory centers, and peripheral, arterial blood baroreceptors and respiratory movements [7]. Analysis of these induced fluctuations allows the assessment of the activity of the central oscillators, the sympathetic and vagal efferent outflow, humoral factors and the sinus node.

HRV power spectrum, during short time analysis, consists of the following spectral components [1]:

- *VLF, very low frequency* (range below 0.04 Hz). The nonharmonic component with no coherent properties, affected by algorithms and baseline or trend removal, is commonly accepted as a major constituent.
- *LF, low frequency* (range from 0.04 to 0.15 Hz). Some studies suggest that LF, when expressed in normalized units, is a quantitative marker of sympathetic modulations, other studies consider LF as reflecting both sympathetic and vagal activity [8].
- *HF, high frequency* (range from 0.15 to 0.4 Hz). The vagal activity is considered the major contributor. This component is in synchrony with the respiration rate, in the range 0.18 to 0.4 Hz, and it is considered to be an expression of the respiration disturbances mediated by the vagal activity [3], [6].

Spectral analysis of HRV represents a challenging alternative for statistical and geometrical measurements from the time domain analysis. The analysis of transient episodes in the heart rate

variability systems allows the evaluation of the sympato-vagal balance in relation with the stimulus onset. The performance with respect of time and frequency resolution of improved versions of the Wigner-Ville Distribution has been tested for a signal simulating a sudden change in spectral components specific to HRV. An example of HRV spectral analysis during the tilt-up test was performed.

## 2. Methods

### 2.1 Quadratic time-frequency representations - theoretical considerations

TFR can be a linear or quadratic (bilinear) function of signal [9]. Among the linear TFRs are the Short Time Fourier Transform, STFT, and the time-frequency version of the Wavelet Transform, WT. The linearity of a TFR is a desirable propriety, but the quadratic structure has a closer interpretation to a time-frequency energy distribution, taking into account that the energy is a quadratic function of signal [9], [10].

The relations between the concept of instantaneous power $p_x(t) = |x(t)^2|$, the spectral energy density $P_x(f)=|X(f)^2|$ and the "energetic" TFR are given by the marginal properties:

$$\int_f T_x(t,f)\,df = p_x(t) = |x(t)|^2 \quad (1)$$

$$\int_t T_x(t,f)\,dt = P_x(f) = |X(f)|^2 \quad (2)$$

As a consequence, the signal energy $E_x$ can be derived by integrating $T_x(t,f)$ over the entire time-frequency plane (3):

$$E_x = \int_t |x(t)|^2\,dt = \int_f |X(f)|^2\,df = \iint_{t,f} T_x(t,f)\,dt\,df$$

The relations (1), (2) don't warrant the interpretation of $T_x(t,f)$ as a "time-frequency energy density" at every point in the time-frequency plane. This is due to the uncertainty principle, which states that the energy of the signal cannot be known with any small time and frequency resolution [9], [10].

The linearity property of a TFR allows the use of the superposition principle: the sum of two signals $x_1$, $x_2$ is the sum of their TFRs, $T_{x1}$ and $T_{x2}$. The same principle cannot be applied to quadratic TFRs. The quadratic superposition principle, in the case of a N-component $x(t) = \sum_k c_k x_k(t)$ states that:

- to each signal component $c_k x_k(t)$ corresponds an auto-component $|c_k|^2 T_{xk}(t,f)$, the auto-term,
- to each pair of signal components $c_k x_k(t)$ and $c_l x_l(t)$, $k \neq l$, corresponds a cross-component $c_k c_l^* T_{xk,xl}(t,f) + c_l c_k^* T_{xl,xk}(t,f)$, the cross-term. The complex conjugate is denoted by the symbol $^*$.

The analysis of a N-component signal is more difficult to interpret as N rises. TFR will consist of N signal terms and N(N-1)/2 interference terms.

Wigner-Ville Distribution, WVD, has very good time-frequency resolution but substantial interference terms.

$$WVD_x(t,f) = \int_t x(t+\frac{\tau}{2})x^*(t-\frac{\tau}{2})e^{-j2\pi ft}\,d\tau \quad (4)$$

where:

$$R_x(t,\tau) = x(t+\frac{\tau}{2})x^*(t-\frac{\tau}{2}) \quad (5)$$

is the instantaneous autocorrelation of the complex signal x(t). Analogous, but with a different physical meaning, the symmetrical ambiguity function, AF, is defined as the inverse Fourier Transform of the instantaneous autocorrelation function, with respect to the time variable t:

$$AF_x(\theta,\tau) = \int_t R_x(t,\tau)e^{j2\pi\theta t}\,dt \quad (6)$$

Thus, the WD and AF are related through the two-dimensional Fourier Transform:

$$WVD_x(t,f) = \iint_{\theta,\tau} AF_x(\theta,\tau)e^{-j2\pi(t\theta+f\tau)}\,d\theta\,d\tau \quad (6)$$

The interference geometry analysis in the ambiguity domain shows a concentration of the auto-terms around the origin and a spread of the interference terms away from origin. This conclusion allows designing of a weighting kernel $\Phi(\theta,\tau)$ in the ambiguity domain, and the generalized Cohen's class of TFRs is given by:

$$C_x(t,f) = \iint_{\theta,\tau} \Phi(\theta,\tau)AF(\theta,\tau)e^{-j2\pi(\theta t+f\tau)}\,d\theta\,d\tau \quad (7)$$

The kernel should have the shape of a 2D low pass filter, thus, the auto-terms around the origin in the ambiguity domain are less weighted than the cross-terms located away from origin.

Choi-William TFR, CW, has the exponential kernel

$$\Phi_{CW}(\theta,\tau) = e^{-\frac{\theta^2\tau^2}{\sigma}} \quad (8)$$

The $\sigma$ parameter, the volume, sets the "cut-off frequency" of the low pass filter, its value being a compromise between the degree of cross-terms canceling and auto-terms smoothing [13]. Some signals that have frequency modulated components

have the auto-terms geometry along a specific angle, away from axis [11], [12], [13], [15]. Such signals require another shape of the kernel, or the increase of the volume on the cost of cross-terms presence.

The interference geometry depends on the signal. Better results can be obtained if the kernel, under some constraints, like a fix volume of the passing region, changes its shape according to this geometry.

The Signal-dependent radially Gaussian kernel TFR, SD, has the following kernel [11], [12]:

$$\Phi_{SD}(\theta,\tau) = e^{-\frac{\theta^2+\tau^2}{2\sigma^2(\Psi)}} \quad (9)$$

where $\sigma(\Psi)$ is called the spread function, controlling the "spread" of the Gaussian at radial angle $\Psi$,

$$\Psi = \arctan\frac{\tau}{\theta} \quad (10)$$

The spread function determines the basic shape of the equal energy contours of the kernel. If the kernel is expressed in polar coordinates, with $r = \sqrt{\theta^2+\tau^2}$

$$\Phi_{SDp}(r,\Psi) = e^{-\frac{r^2}{2\sigma^2(\Psi)}} \quad (11)$$

The kernel shape is parameterized by the one-dimensional function $\sigma(\Psi)$. Finding the optimal radially Gaussian kernel for a signal is equivalent with finding the optimal spread function $\sigma_{opt}(\Psi)$. The optimization problem is given by:

$$\max_{\Psi}\int_0^{2\pi}\int_0^{\infty}\left|AF(r,\Psi)\Phi(r,\Psi)\right|^2 r dr d\Psi \quad (12)$$

with the following constraint:

$$\frac{1}{2\pi}\int_0^{2\pi}\int_0^{\infty}\left|\Phi(r,\Psi)\right|^2 r dr d\Psi \le \alpha\,, \qquad \alpha \ge 0, \quad (13)$$

which can be written as:

$$\int_0^{2\pi}\int_0^{\infty}\sigma(\psi)^2 d\Psi \le \alpha\,, \quad (14)$$

This is equivalent to a fix volume of kernel in the ambiguity domain. The solution is found by using a similar method with the gradient-projection algorithm [11].

### 2.2 Simulated and real HRV data

Two simulated signals were computed as:

a) $x_1[n] = e^{-j2\pi f_1 n} + e^{-j2\pi f 2n} + e^{-j2\pi f 3n}$ (15)

n = 1..64 sec, $f_1$ = 0.04 Hz, $f_2$ = 0.12 Hz, $f_3$ = 0.25 Hz,

b) $x_2[n] = e^{-j2\pi f_1 n} + e^{-j2\pi f_2 n} + e^{-j2\pi f_3 n}$, (16)

n = 1..32 sec, $f_1$ = 0.04 Hz, $f_2$ = 0.15 Hz, $f_3$ = 0.3 Hz

$x_2[n] = e^{-j2\pi f_1 n} + e^{-j2\pi f_2 n} + e^{-j2\pi f_3 n}$,

n = 33..64 sec, $f_1$ = 0.12 Hz, $f_2$ = 0.2 Hz, $f_3$ = 0.4 Hz,

having a spectrum corresponding to the VLF, LF and HF components specific to HRV.

The CW kernel (Fig.1C) had a symmetric geometry concentrated along the axis and around the center of

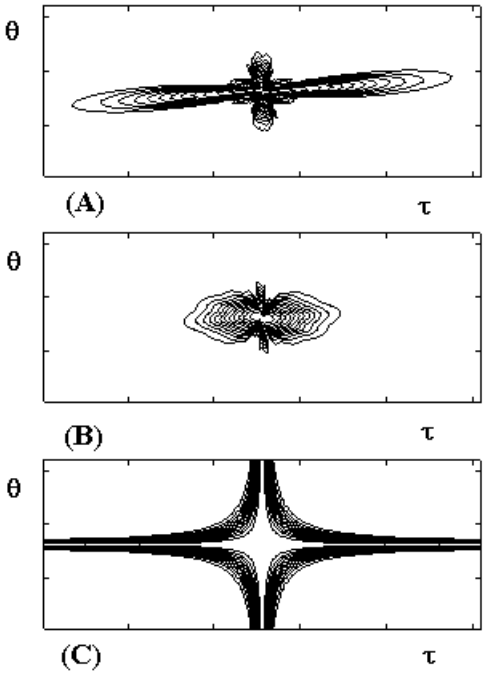


**Fig. 1** The kernels for SD: (A) $x_1$, (B) $x_2$ with $\alpha = 4$, the number of iteration for optimization problem N = 60, and for CW: (C) $x_1$ and $x_2$, with $\sigma = 4$.

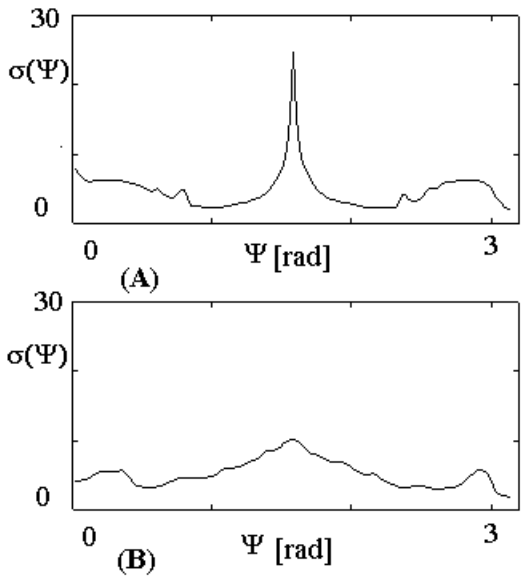


**Fig. 2** The spread function: (A) $x_1$ and (B) $x_2$.

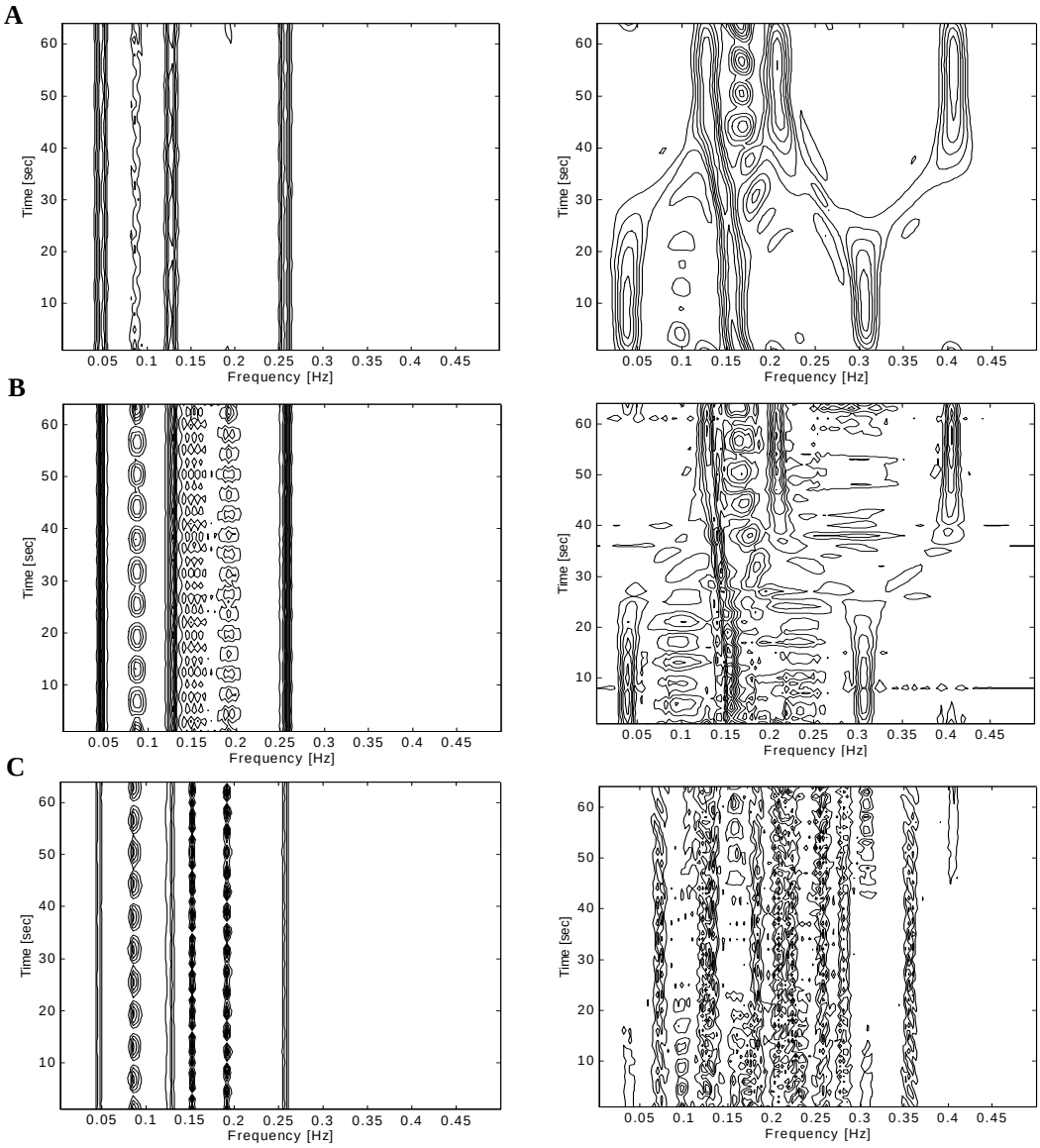


**Fig. 3** Simulated HRV analysis with Wigner-Ville Distribution (C), Choi-William TFR (B) and Signal-dependent radially Gaussian kernel TFR (A) for the cases: (left) signal $x_1$ with no time change spectrum, with frequency components located at 0.04, 0.12 and 0.25 Hz; (right) signal $x_2$, with spectrum change at time = 32 s from frequency components located at 0.03, 0.15, 0.3 Hz to 0.12, 0.2, 0.4 Hz ; the same volume parameter of the filter ($\sigma$ = 4 for CW and $\alpha$=4 for SD) and the iteration number for the optimization problem N = 60.

the ambiguity domain. The SD kernels corresponding to $x_1$ and $x_2$ signals (Fig.1A and B) had variable geometry depending on the signal components. This geometry was given by the solution of the optimization problem, the spread function (Fig.2A and B). In the case of $x_1$ there was no change in the spectrum and the shape of the kernel tends to be closer to axis, similar to the CW kernel, whereas a higher concentration around the center rather than a spread along the axis could be noticed due to a change in frequency after a time of 32 s.

Two sets of ECG recordings, corresponding to the clinostatic position (r1) and the orthostatic position (r2) were analysed. The ECG was sampled with 256 Hz. The RR intervals (NN normal to normal series, expressed in ms) were extracted and cubic spline interpolated at 250 ms. An analytic signal, which has no components at negative frequencies in the spectrum, was computed from the interpolated series. This contributes to a reduced number of cross-terms by avoiding the pairs with components at negative frequencies in the WVD.

## 3. Results

In Fig.3 are presented the WVD, CW, and SD for the simulated HRV signals. WVD has a very good frequency resolution but the cross-terms make almost impossible the interpretation in the case of

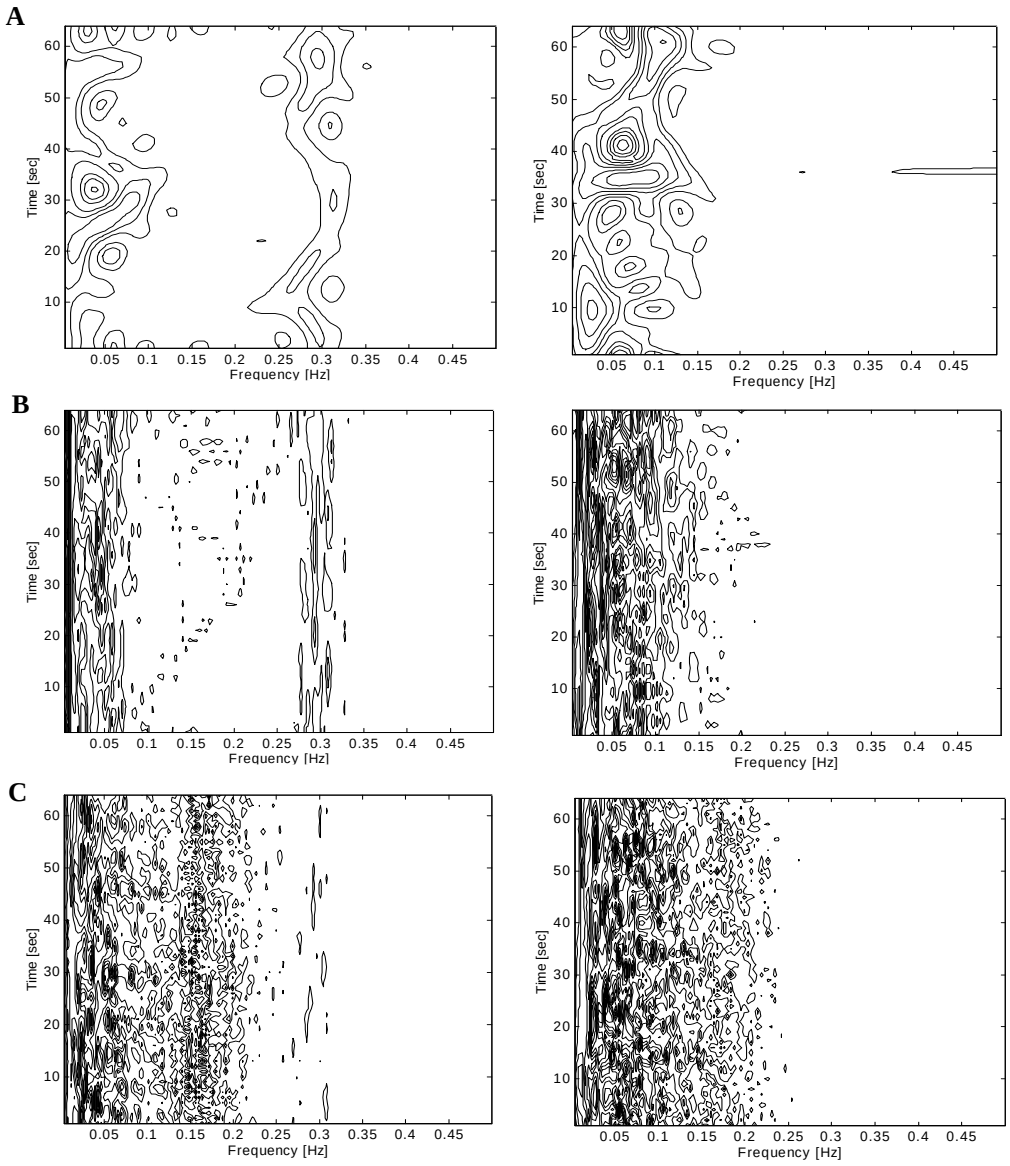


**Fig. 4** HRV (RR intervals) analysis with Wigner-Ville Distribution (C), Choi-William TFR (B) and Radially Gaussian Kernel Signal- dependent radially Gaussian kernel (A) TFRs for: (left) r1 recording, orthostatic position, (right) r2 recording, clinostatic position; the same volume parameter of the filter ($\sigma$ = 4 for CW and $\alpha$=4 for SD) and the iteration number for the optimization problem N = 60.

the signal $x_2$. Any processing in the ambiguity domain results in a decrease in frequency resolution, obtaining an auto-terms smearing, as can be seen in the case of CW and more in the case of SD.

The auto-terms can be identified at 0.04, 0.12 and 0.25 Hz in the WVD of the signal x1. The cross-terms are characterized by time oscillations and they are located in the middle of a pair of auto-terms, with respect with frequency. CW of the signal $x_1$ has a lower frequency resolution than WVD and the cross-terms are canceled in a degree between 40 and 73%. This degree can be improved if the volume of the CW kernel is decreased, but with the cost of the auto-terms smoothing. SD of the signal $x_1$ has very good cross-terms canceling degree (up to 100%), but the frequency resolution is further decreased.

In the WVD of the signal $x_2$ is very difficult to identify the auto-terms. The most "readable" TFR for the signal $x_2$ is the SD, followed by CW. The spectral components can be easily identified. The sudden transition at the time of 32 s is well represented in CW and SD (with a slight improvement) and impossible to detect in WVD.

The analysis of two data series of the interpolated RR intervals obtained from ECG recordings is shown in Fig.4. The clinostatic position (r1, Fig.4 left) is characterized by an elevated vagal (high HF component around 0.3 Hz) and reduced sympathetic (relative low LF between 0.05 and 0.1 Hz) activity. The tilt-up to the orthostatic position changes the balance in the autonomic nervous control of the heart (r2, Fig.4 right) by reducing the vagal

component (HF) and increasing in sympathetic component (LF). The performance of CW relative to SD is similar with case of the simulated signals.

## 4. Conclusion

In this work was presented the application of three known time-frequency representations, Wigner-Ville Distribution, Choi-William TFR and Signal-dependent TFR with radially Gaussian kernel for heart rate variability analysis. The simulation and case study showed that the performances of the WVD could be improved by using a weighting kernel in the ambiguity domain. CW TFR and SD TFR have comparative results, both of them presenting advantages and disadvantages like trade-off between auto-terms smearing and cross-terms canceling.

*References*

[1] Special Report, Heart Rate Variability. Standards of Measurement, Physiological Interpretation and Clinical Use, Task Force of the European Society of Cardiology and the North American Society of Pacing and Electrophysiology, *Circulation*, Vol. 93, No. 5, 1996, pp. 1043-1065.

[2] S. Pola, A. Macerata, Estimation of the Power Spectral Density in Nonstationary Cardiovascular Time Series. Assessing the Role of the Time-Frequency Representations, *IEEE Trans. On BME*, Vol. 43, No. 1, 1996, pp. 46-59.

[3] P. Stein, M. Bosner, Heart Rate Variability. A measure of Cardiac Autonomic Tone, *American Heart Journal*, Vol. 127, No. 5, 1992, pp. 1376-1381.

[4] F. Bellavere, I. Balzani, S. de Masi, Power Spectral Analysis of Heart Rate Variations Improves Assessment of Diabetic Cardiac Autonomic Neuropathy *Diabetes*, Vol. 41, No. 5, 1992, pp. 633-640.

[5] F. Lombardi, G. Sandrone, M. Teresa Spinnler, Heart Rate Variability in the Early Hours of an Acute Myocardial Infarction, *Am. J. of Cardiology*, Vol. 77, 1996, pp. 1037-1044.

[6] A. Malliani, F. Lombardi, M. Pagani, Power spectrum Analysis of Heart Rate Variability. A Tool to Explore neural Regulatory Mechanisms, *British Heart Journal*, Vol. 71, 1994, pp. 1-3.

[7] A. Bianchi, L. Mainardi, E Petrucci, Time-Variant Power Spectrum Analysis for the detection of Transient Episodes in HRV Signal, *IEEE Trans. on BME*, Vol. 40, No. 2, 1993, pp. 136-144.

[8] F. Lombardi, G. Sandrone, S. Pernpruner, Heart Rate Variability as an Index of Simpatovagal Interaction After Acute Myocardial Infarction, *Am J. of Cardiology*, Vol. 60, 1987, pp. 1239-1245.

[9] F. Hlawatsch, F. Boudreaux-Bartels, Linear and Quadratic Time-Frequency Signal Representations, *IEEE Sp. Magazine* 1992, pp. 21-67.

[10] L. Cohen, Time-Frequency Distribution. A Review, *Proc. of the IEEE*, Vol. 77, No, 7, 1989, pp. 941-981.

[11] R. Baraniuk, D. Jones, Signal Dependent Time-Frequency Analysis Using a Radially Gaussian Kernel, *Signal Processing*, Vol. 32, 1993, pp. 263-284.

[12] D. Jones, R. Baraniuk, An Adaptive Optimal-Kernel Time-Frequency Representations, *IEEE Trans. on SP*, Vol. 43, No. 10, 1995, pp. 2361-2371.

[13] H. Choi, W. Williams, Improved Time-Frequency Representations of Multicomponent Signals Using Exponential Kernels, *IEEE Trans. on ASSP*, Vol. 37, No. 6, 1989, pp. 862-870.

[14] Y. Zhao, L. Atlas, R. Marks, The Use of the Cone-Shaped Kernels for Generalised Time-Frequency Representations of Nonstationary Signals, *IEEE Trans. on ASSP*, Vol. 38, No. 7, 1990, pp. 1084-1091.

[15] J. Jeong, W. Williams, Kernel Design for Reduced Interference Distributions. *IEEE Trans. on SP*, Vol. 40, No. 2, 1992, pp. 402-412.

[16] J. Sztajzel, Heart rate variability: a noninvasive electrocardiographic method to measure the autonomic nervous system. *Swiss Med Wkly*., Vol. 134, No. 35-36, 2004, pp. 514-522.

[17] O. Faust, U.R. Acharya, S.M. Krishnan, L.C. Min. Analysis of cardiac signals using spatial filling index and time-frequency domain. *Biomed Eng Online*, 3(1):30, 10 Sep 2004.

[18] D. Wichterle, J. Simek, M.T. La Rovere, P.J. Schwartz, A.J. Camm, M. Malik. Prevalent low-frequency oscillation of heart rate: novel predictor of mortality after myocardial infarction. *Circulation*, Vol. 110, No. 10, 2004, pp. 1183-90.